

Measurements of the Angular Distributions in the Decays $B \rightarrow K^{(*)}\mu^+\mu^-$ at CDF

T. Aaltonen,²² B. Álvarez González^v,¹⁰ S. Amerio,⁴² D. Amidei,³³ A. Anastassov,³⁷ A. Annovi,¹⁸ J. Antos,¹³ G. Apollinari,¹⁶ J.A. Appel,¹⁶ A. Apresyan,⁴⁷ T. Arisawa,⁵⁶ A. Artikov,¹⁴ J. Asaadi,⁵² W. Ashmanskas,¹⁶ B. Auerbach,⁵⁹ A. Aurisano,⁵² F. Azfar,⁴¹ W. Badgett,¹⁶ A. Barbaro-Galtieri,²⁷ V.E. Barnes,⁴⁷ B.A. Barnett,²⁴ P. Barria^{ee},⁴⁵ P. Bartos,¹³ M. Bauce^{cc},⁴² G. Bauer,³¹ F. Bedeschi,⁴⁵ D. Beecher,²⁹ S. Behari,²⁴ G. Bellettini^{dd},⁴⁵ J. Bellinger,⁵⁸ D. Benjamin,¹⁵ A. Beretvas,¹⁶ A. Bhatti,⁴⁹ M. Binkley^{*},¹⁶ D. Bisello^{cc},⁴² I. Bizjakⁱⁱ,²⁹ K.R. Bland,⁵ C. Blocker,⁷ B. Blumenfeld,²⁴ A. Bocci,¹⁵ A. Bodek,⁴⁸ D. Bortoletto,⁴⁷ J. Boudreau,⁴⁶ A. Boveia,¹² B. Brau^a,¹⁶ L. Brigliadori^{bb},⁶ A. Brisuda,¹³ C. Bromberg,³⁴ E. Brucken,²² M. Bucciantonio^{dd},⁴⁵ J. Budagov,¹⁴ H.S. Budd,⁴⁸ S. Budd,²³ K. Burkett,¹⁶ G. Busetto^{cc},⁴² P. Bussey,²⁰ A. Buzatu,³² S. Cabrera^x,¹⁵ C. Calancha,³⁰ S. Camarda,⁴ M. Campanelli,³⁴ M. Campbell,³³ F. Canelli¹²,¹⁶ A. Canepa,⁴⁴ B. Carls,²³ D. Carlsmith,⁵⁸ R. Carosi,⁴⁵ S. Carrillo^k,¹⁷ S. Carron,¹⁶ B. Casal,¹⁰ M. Casarsa,¹⁶ A. Castro^{bb},⁶ P. Catastini,¹⁶ D. Cauz,⁵³ V. Cavaliere^{ee},⁴⁵ M. Cavalli-Sforza,⁴ A. Cerri^f,²⁷ L. Cerrito^q,²⁹ Y.C. Chen,¹ M. Chertok,⁸ G. Chiarelli,⁴⁵ G. Chlachidze,¹⁶ F. Chlebana,¹⁶ K. Cho,²⁶ D. Chokheli,¹⁴ J.P. Chou,²¹ W.H. Chung,⁵⁸ Y.S. Chung,⁴⁸ C.I. Ciobanu,⁴³ M.A. Ciocci^{ee},⁴⁵ A. Clark,¹⁹ D. Clark,⁷ G. Compostella^{cc},⁴² M.E. Convery,¹⁶ J. Conway,⁸ M. Corbo,⁴³ M. Cordelli,¹⁸ C.A. Cox,⁸ D.J. Cox,⁸ F. Crescioli^{dd},⁴⁵ C. Cuenca Almenar,⁵⁹ J. Cuevas^v,¹⁰ R. Culbertson,¹⁶ D. Dagenhart,¹⁶ N. d'Ascenzo^t,⁴³ M. Datta,¹⁶ P. de Barbaro,⁴⁸ S. De Cecco,⁵⁰ G. De Lorenzo,⁴ M. Dell'Orso^{dd},⁴⁵ C. Deluca,⁴ L. Demortier,⁴⁹ J. Deng^c,¹⁵ M. Deninno,⁶ F. Devoto,²² M. d'Errico^{cc},⁴² A. Di Canto^{dd},⁴⁵ B. Di Ruzza,⁴⁵ J.R. Dittmann,⁵ M. D'Onofrio,²⁸ S. Donati^{dd},⁴⁵ P. Dong,¹⁶ T. Dorigo,⁴² K. Ebina,⁵⁶ A. Elagin,⁵² A. Eppig,³³ R. Erbacher,⁸ D. Errede,²³ S. Errede,²³ N. Ershaidat^{aa},⁴³ R. Eusebi,⁵² H.C. Fang,²⁷ S. Farrington,⁴¹ M. Feindt,²⁵ J.P. Fernandez,³⁰ C. Ferrazza^{ff},⁴⁵ R. Field,¹⁷ G. Flanagan^r,⁴⁷ R. Forrest,⁸ M.J. Frank,⁵ M. Franklin,²¹ J.C. Freeman,¹⁶ I. Furic,¹⁷ M. Gallinaro,⁴⁹ J. Galyardt,¹¹ J.E. Garcia,¹⁹ A.F. Garfinkel,⁴⁷ P. Garosi^{ee},⁴⁵ H. Gerberich,²³ E. Gerchtein,¹⁶ S. Giagu^{gg},⁵⁰ V. Giakoumopoulou,³ P. Giannetti,⁴⁵ K. Gibson,⁴⁶ C.M. Ginsburg,¹⁶ N. Giokaris,³ P. Giromini,¹⁸ M. Giunta,⁴⁵ G. Giurgiu,²⁴ V. Glagolev,¹⁴ D. Glenzinski,¹⁶ M. Gold,³⁶ D. Goldin,⁵² N. Goldschmidt,¹⁷ A. Golossanov,¹⁶ G. Gomez,¹⁰ G. Gomez-Ceballos,³¹ M. Goncharov,³¹ O. González,³⁰ I. Gorelov,³⁶ A.T. Goshaw,¹⁵ K. Goulianos,⁴⁹ A. Gresele,⁴² S. Grinstein,⁴ C. Grosso-Pilcher,¹² R.C. Group,¹⁶ J. Guimaraes da Costa,²¹ Z. Gunay-Unalan,³⁴ C. Haber,²⁷ S.R. Hahn,¹⁶ E. Halkiadakis,⁵¹ A. Hamaguchi,⁴⁰ J.Y. Han,⁴⁸ F. Happacher,¹⁸ K. Hara,⁵⁴ D. Hare,⁵¹ M. Hare,⁵⁵ R.F. Harr,⁵⁷ K. Hatakeyama,⁵ C. Hays,⁴¹ M. Heck,²⁵ J. Heinrich,⁴⁴ M. Herndon,⁵⁸ S. Hewamanage,⁵ D. Hidas,⁵¹ A. Hocker,¹⁶ W. Hopkins^g,¹⁶ D. Horn,²⁵ S. Hou,¹ R.E. Hughes,³⁸ M. Hurwitz,¹² U. Husemann,⁵⁹ N. Hussain,³² M. Hussein,³⁴ J. Huston,³⁴ G. Introzzi,⁴⁵ M. Iori^{gg},⁵⁰ A. Ivanov^o,⁸ E. James,¹⁶ D. Jang,¹¹ B. Jayatilaka,¹⁵ E.J. Jeon,²⁶ M.K. Jha,⁶ S. Jindariani,¹⁶ W. Johnson,⁸ M. Jones,⁴⁷ K.K. Joo,²⁶ S.Y. Jun,¹¹ T.R. Junk,¹⁶ T. Kamon,⁵² P.E. Karchin,⁵⁷ Y. Katoⁿ,⁴⁰ W. Ketchum,¹² J. Keung,⁴⁴ V. Khotilovich,⁵² B. Kilminster,¹⁶ D.H. Kim,²⁶ H.S. Kim,²⁶ H.W. Kim,²⁶ J.E. Kim,²⁶ M.J. Kim,¹⁸ S.B. Kim,²⁶ S.H. Kim,⁵⁴ Y.K. Kim,¹² N. Kimura,⁵⁶ S. Klimenko,¹⁷ K. Kondo,⁵⁶ D.J. Kong,²⁶ J. Konigsberg,¹⁷ A. Korytov,¹⁷ A.V. Kotwal,¹⁵ M. Kreps,²⁵ J. Kroll,⁴⁴ D. Krop,¹² N. Krumnack^l,⁵ M. Kruse,¹⁵ V. Krutiyov^d,⁵² T. Kuhr,²⁵ M. Kurata,⁵⁴ S. Kwang,¹² A.T. Laasanen,⁴⁷ S. Lami,⁴⁵ S. Lammel,¹⁶ M. Lancaster,²⁹ R.L. Lander,⁸ K. Lannon^u,³⁸ A. Lath,⁵¹ G. Latino^{ee},⁴⁵ I. Lazzizzera,⁴² T. LeCompte,² E. Lee,⁵² H.S. Lee,¹² J.S. Lee,²⁶ S.W. Lee^w,⁵² S. Leo^{dd},⁴⁵ S. Leone,⁴⁵ J.D. Lewis,¹⁶ C.-J. Lin,²⁷ J. Linacre,⁴¹ M. Lindgren,¹⁶ E. Lipeles,⁴⁴ A. Lister,¹⁹ D.O. Litvintsev,¹⁶ C. Liu,⁴⁶ Q. Liu,⁴⁷ T. Liu,¹⁶ S. Lockwitz,⁵⁹ N.S. Lockyer,⁴⁴ A. Loginov,⁵⁹ D. Lucchesi^{cc},⁴² J. Lueck,²⁵ P. Lujan,²⁷ P. Lukens,¹⁶ G. Lungu,⁴⁹ J. Lys,²⁷ R. Lysak,¹³ R. Madrak,¹⁶ K. Maeshima,¹⁶ K. Makhoul,³¹ P. Maksimovic,²⁴ S. Malik,⁴⁹ G. Manca^b,²⁸ A. Manousakis-Katsikakis,³ F. Margaroli,⁴⁷ C. Marino,²⁵ M. Martínez,⁴ R. Martínez-Ballarín,³⁰ P. Mastrandrea,⁵⁰ M. Mathis,²⁴ M.E. Mattson,⁵⁷ P. Mazzanti,⁶ K.S. McFarland,⁴⁸ P. McIntyre,⁵² R. McNultyⁱ,²⁸ A. Mehta,²⁸ P. Mehtala,²² A. Menzione,⁴⁵ C. Mesropian,⁴⁹ T. Miao,¹⁶ D. Mietlicki,³³ A. Mitra,¹ H. Miyake,⁵⁴ S. Moed,²¹ N. Moggi,⁶ M.N. Mondragon^k,¹⁶ C.S. Moon,²⁶ R. Moore,¹⁶ M.J. Morello,¹⁶ J. Morlock,²⁵ P. Movilla Fernandez,¹⁶ A. Mukherjee,¹⁶ Th. Muller,²⁵ P. Murat,¹⁶ M. Mussini^{bb},⁶ J. Nachtman^m,¹⁶ Y. Nagai,⁵⁴ J. Naganoma,⁵⁶ I. Nakano,³⁹ A. Napier,⁵⁵ J. Nett,⁵⁸ C. Neu^z,⁴⁴ M.S. Neubauer,²³ J. Nielsen^e,²⁷ L. Nodulman,² O. Norriella,²³ E. Nurse,²⁹ L. Oakes,⁴¹ S.H. Oh,¹⁵ Y.D. Oh,²⁶ I. Oksuzian,¹⁷ T. Okusawa,⁴⁰ R. Orava,²² L. Ortolan,⁴ S. Pagan Griso^{cc},⁴² C. Pagliarone,⁵³ E. Palencia^f,¹⁰ V. Papadimitriou,¹⁶ A.A. Paramonov,² J. Patrick,¹⁶ G. Pauletta^{hh},⁵³ M. Paulini,¹¹ C. Paus,³¹ D.E. Pellett,⁸ A. Penzo,⁵³ T.J. Phillips,¹⁵ G. Piacentino,⁴⁵ E. Pianori,⁴⁴ J. Pilot,³⁸ K. Pitts,²³ C. Plager,⁹ L. Pondrom,⁵⁸ K. Potamianos,⁴⁷ O. Poukhov^{*},¹⁴ F. Prokoshin^y,¹⁴ A. Pronko,¹⁶ F. Ptohos^h,¹⁸ E. Pueschel,¹¹ G. Punzi^{dd},⁴⁵ J. Pursley,⁵⁸ A. Rahaman,⁴⁶ V. Ramakrishnan,⁵⁸ N. Ranjan,⁴⁷ I. Redondo,³⁰ P. Renton,⁴¹ M. Rescigno,⁵⁰

F. Rimondi^{bb},⁶ L. Ristori⁴⁵,¹⁶ A. Robson,²⁰ T. Rodrigo,¹⁰ T. Rodriguez,⁴⁴ E. Rogers,²³ S. Rolli,⁵⁵ R. Roser,¹⁶ M. Rossi,⁵³ F. Ruffini^{ee},⁴⁵ A. Ruiz,¹⁰ J. Russ,¹¹ V. Rusu,¹⁶ A. Safonov,⁵² W.K. Sakumoto,⁴⁸ L. Santi^{hh},⁵³ L. Sartori,⁴⁵ K. Sato,⁵⁴ V. Saveliev^t,⁴³ A. Savoy-Navarro,⁴³ P. Schlabach,¹⁶ A. Schmidt,²⁵ E.E. Schmidt,¹⁶ M.P. Schmidt^{*},⁵⁹ M. Schmitt,³⁷ T. Schwarz,⁸ L. Scodellaro,¹⁰ A. Scribano^{ee},⁴⁵ F. Scuri,⁴⁵ A. Sedov,⁴⁷ S. Seidel,³⁶ Y. Seiya,⁴⁰ A. Semenov,¹⁴ F. Sforza^{dd},⁴⁵ A. Sfyrlla,²³ S.Z. Shalhout,⁸ T. Shears,²⁸ P.F. Shepard,⁴⁶ M. Shimojima^s,⁵⁴ S. Shiraishi,¹² M. Shochet,¹² I. Shreyber,³⁵ A. Simonenko,¹⁴ P. Sinervo,³² A. Sissakian^{*},¹⁴ K. Sliwa,⁵⁵ J.R. Smith,⁸ F.D. Snider,¹⁶ A. Soha,¹⁶ S. Somalwar,⁵¹ V. Sorin,⁴ P. Squillacioti,¹⁶ M. Stanitzki,⁵⁹ R. St. Denis,²⁰ B. Stelzer,³² O. Stelzer-Chilton,³² D. Stentz,³⁷ J. Strologas,³⁶ G.L. Strycker,³³ Y. Sudo,⁵⁴ A. Sukhanov,¹⁷ I. Suslov,¹⁴ K. Takemasa,⁵⁴ Y. Takeuchi,⁵⁴ J. Tang,¹² M. Tecchio,³³ P.K. Teng,¹ J. Thom^g,¹⁶ J. Thome,¹¹ G.A. Thompson,²³ E. Thomson,⁴⁴ P. Ttito-Guzmán,³⁰ S. Tkaczyk,¹⁶ D. Toback,⁵² S. Tokar,¹³ K. Tollefson,³⁴ T. Tomura,⁵⁴ D. Tonelli,¹⁶ S. Torre,¹⁸ D. Torretta,¹⁶ P. Totaro^{hh},⁵³ M. Trovato^{ff},⁴⁵ Y. Tu,⁴⁴ N. Turini^{ee},⁴⁵ F. Ukegawa,⁵⁴ S. Uozumi,²⁶ A. Varganov,³³ E. Vataga^{ff},⁴⁵ F. Vázquez^k,¹⁷ G. Velez,¹⁶ C. Vellidis,³ M. Vidal,³⁰ I. Vila,¹⁰ R. Vilar,¹⁰ M. Vogel,³⁶ G. Volpi^{dd},⁴⁵ P. Wagner,⁴⁴ R.L. Wagner,¹⁶ T. Wakisaka,⁴⁰ R. Wallny,⁹ S.M. Wang,¹ A. Warburton,³² D. Waters,²⁹ M. Weinberger,⁵² H. Wenzel,¹⁶ W.C. Wester III,¹⁶ B. Whitehouse,⁵⁵ D. Whiteson^c,⁴⁴ A.B. Wicklund,² E. Wicklund,¹⁶ S. Wilbur,¹² F. Wick,²⁵ H.H. Williams,⁴⁴ J.S. Wilson,³⁸ P. Wilson,¹⁶ B.L. Winer,³⁸ P. Wittich^g,¹⁶ S. Wolbers,¹⁶ H. Wolfe,³⁸ T. Wright,³³ X. Wu,¹⁹ Z. Wu,⁵ K. Yamamoto,⁴⁰ J. Yamaoka,¹⁵ T. Yang,¹⁶ U.K. Yang^p,¹² Y.C. Yang,²⁶ W.-M. Yao,²⁷ G.P. Yeh,¹⁶ K. Yi^m,¹⁶ J. Yoh,¹⁶ K. Yorita,⁵⁶ T. Yoshida^j,⁴⁰ G.B. Yu,¹⁵ I. Yu,²⁶ S.S. Yu,¹⁶ J.C. Yun,¹⁶ A. Zanetti,⁵³ Y. Zeng,¹⁵ and S. Zucchelli^{bb6}

(CDF Collaboration[†])

¹*Institute of Physics, Academia Sinica, Taipei, Taiwan 11529, Republic of China*

²*Argonne National Laboratory, Argonne, Illinois 60439, USA*

³*University of Athens, 157 71 Athens, Greece*

⁴*Institut de Fisica d'Altes Energies, Universitat Autònoma de Barcelona, E-08193, Bellaterra (Barcelona), Spain*

⁵*Baylor University, Waco, Texas 76798, USA*

⁶*Istituto Nazionale di Fisica Nucleare Bologna, ^{bb}University of Bologna, I-40127 Bologna, Italy*

⁷*Brandeis University, Waltham, Massachusetts 02254, USA*

⁸*University of California, Davis, Davis, California 95616, USA*

⁹*University of California, Los Angeles, Los Angeles, California 90024, USA*

¹⁰*Instituto de Fisica de Cantabria, CSIC-University of Cantabria, 39005 Santander, Spain*

¹¹*Carnegie Mellon University, Pittsburgh, Pennsylvania 15213, USA*

¹²*Enrico Fermi Institute, University of Chicago, Chicago, Illinois 60637, USA*

¹³*Comenius University, 842 48 Bratislava, Slovakia; Institute of Experimental Physics, 040 01 Kosice, Slovakia*

¹⁴*Joint Institute for Nuclear Research, RU-141980 Dubna, Russia*

¹⁵*Duke University, Durham, North Carolina 27708, USA*

¹⁶*Fermi National Accelerator Laboratory, Batavia, Illinois 60510, USA*

¹⁷*University of Florida, Gainesville, Florida 32611, USA*

¹⁸*Laboratori Nazionali di Frascati, Istituto Nazionale di Fisica Nucleare, I-00044 Frascati, Italy*

¹⁹*University of Geneva, CH-1211 Geneva 4, Switzerland*

²⁰*Glasgow University, Glasgow G12 8QQ, United Kingdom*

²¹*Harvard University, Cambridge, Massachusetts 02138, USA*

²²*Division of High Energy Physics, Department of Physics, University of Helsinki and Helsinki Institute of Physics, FIN-00014, Helsinki, Finland*

²³*University of Illinois, Urbana, Illinois 61801, USA*

²⁴*The Johns Hopkins University, Baltimore, Maryland 21218, USA*

²⁵*Institut für Experimentelle Kernphysik, Karlsruhe Institute of Technology, D-76131 Karlsruhe, Germany*

²⁶*Center for High Energy Physics: Kyungpook National University,*

Daegu 702-701, Korea; Seoul National University, Seoul 151-742,

Korea; Sungkyunkwan University, Suwon 440-746,

Korea; Korea Institute of Science and Technology Information,

Daejeon 305-806, Korea; Chonnam National University, Gwangju 500-757,

Korea; Chonbuk National University, Jeonju 561-756, Korea

²⁷*Ernest Orlando Lawrence Berkeley National Laboratory, Berkeley, California 94720, USA*

²⁸*University of Liverpool, Liverpool L69 7ZE, United Kingdom*

²⁹*University College London, London WC1E 6BT, United Kingdom*

³⁰*Centro de Investigaciones Energéticas Medioambientales y Tecnológicas, E-28040 Madrid, Spain*

³¹*Massachusetts Institute of Technology, Cambridge, Massachusetts 02139, USA*

³²*Institute of Particle Physics: McGill University, Montréal, Québec,*

Canada H3A 2T8; Simon Fraser University, Burnaby, British Columbia,

- Canada V5A 1S6; University of Toronto, Toronto, Ontario,
Canada M5S 1A7; and TRIUMF, Vancouver, British Columbia, Canada V6T 2A3
- ³³University of Michigan, Ann Arbor, Michigan 48109, USA
- ³⁴Michigan State University, East Lansing, Michigan 48824, USA
- ³⁵Institution for Theoretical and Experimental Physics, ITEP, Moscow 117259, Russia
- ³⁶University of New Mexico, Albuquerque, New Mexico 87131, USA
- ³⁷Northwestern University, Evanston, Illinois 60208, USA
- ³⁸The Ohio State University, Columbus, Ohio 43210, USA
- ³⁹Okayama University, Okayama 700-8530, Japan
- ⁴⁰Osaka City University, Osaka 588, Japan
- ⁴¹University of Oxford, Oxford OX1 3RH, United Kingdom
- ⁴²Istituto Nazionale di Fisica Nucleare, Sezione di Padova-Trento, ^{cc}University of Padova, I-35131 Padova, Italy
- ⁴³LPNHE, Universite Pierre et Marie Curie/IN2P3-CNRS, UMR7585, Paris, F-75252 France
- ⁴⁴University of Pennsylvania, Philadelphia, Pennsylvania 19104, USA
- ⁴⁵Istituto Nazionale di Fisica Nucleare Pisa, ^{dd}University of Pisa,
- ^{ee}University of Siena and ^{ff}Scuola Normale Superiore, I-56127 Pisa, Italy
- ⁴⁶University of Pittsburgh, Pittsburgh, Pennsylvania 15260, USA
- ⁴⁷Purdue University, West Lafayette, Indiana 47907, USA
- ⁴⁸University of Rochester, Rochester, New York 14627, USA
- ⁴⁹The Rockefeller University, New York, New York 10065, USA
- ⁵⁰Istituto Nazionale di Fisica Nucleare, Sezione di Roma 1,
- ^{gg}Sapienza Università di Roma, I-00185 Roma, Italy
- ⁵¹Rutgers University, Piscataway, New Jersey 08855, USA
- ⁵²Texas A&M University, College Station, Texas 77843, USA
- ⁵³Istituto Nazionale di Fisica Nucleare Trieste/Udine,
I-34100 Trieste, ^{hh}University of Trieste/Udine, I-33100 Udine, Italy
- ⁵⁴University of Tsukuba, Tsukuba, Ibaraki 305, Japan
- ⁵⁵Tufts University, Medford, Massachusetts 02155, USA
- ⁵⁶Waseda University, Tokyo 169, Japan
- ⁵⁷Wayne State University, Detroit, Michigan 48201, USA
- ⁵⁸University of Wisconsin, Madison, Wisconsin 53706, USA
- ⁵⁹Yale University, New Haven, Connecticut 06520, USA

We reconstruct the decays $B \rightarrow K^{(*)}\mu^+\mu^-$ and measure their angular distributions in $p\bar{p}$ collisions at $\sqrt{s} = 1.96$ TeV using a data sample corresponding to an integrated luminosity of 6.8 fb^{-1} . The transverse polarization asymmetry $A_T^{(2)}$ and the time-reversal-odd charge-and-parity asymmetry A_{im} are measured for the first time, together with the K^* longitudinal polarization fraction F_L and the muon forward-backward asymmetry A_{FB} , for the decays $B^0 \rightarrow K^{*0}\mu^+\mu^-$ and $B^+ \rightarrow K^{*+}\mu^+\mu^-$. Our results are among the most accurate to date and consistent with those from other experiments.

PACS numbers: 13.25 Hw, 13.20 He

*Deceased

†With visitors from ^aUniversity of Massachusetts Amherst, Amherst, Massachusetts 01003, ^bIstituto Nazionale di Fisica Nucleare, Sezione di Cagliari, 09042 Monserrato (Cagliari), Italy, ^cUniversity of California Irvine, Irvine, CA 92697, ^dUniversity of California Santa Barbara, Santa Barbara, CA 93106 ^eUniversity of California Santa Cruz, Santa Cruz, CA 95064, ^fCERN, CH-1211 Geneva, Switzerland, ^gCornell University, Ithaca, NY 14853, ^hUniversity of Cyprus, Nicosia CY-1678, Cyprus, ⁱUniversity College Dublin, Dublin 4, Ireland, ^jUniversity of Fukui, Fukui City, Fukui Prefecture, Japan 910-0017, ^kUniversidad Iberoamericana, Mexico D.F., Mexico, ^lIowa State University, Ames, IA 50011, ^mUniversity of Iowa, Iowa City, IA 52242, ⁿKinki University, Higashi-Osaka City, Japan 577-8502, ^oKansas State University, Manhattan, KS 66506, ^pUniversity of Manchester, Manchester M13 9PL, England, ^qQueen Mary, University of London, London, E1 4NS, England, ^rMuons, Inc., Batavia, IL 60510, ^sNagasaki Institute of Applied Science, Nagasaki, Japan, ^tNational Research Nuclear University, Moscow, Russia, ^uUniversity of Notre Dame,

The decays $B \rightarrow K^{(*)}\mu^+\mu^-$, which proceed via the flavor-changing neutral-current (FCNC) process $b \rightarrow s\mu\mu$, are considered among the most promising probes of the standard model (SM) and its extensions. In the SM they occur through higher order amplitudes, though additional processes with beyond-the-standard-model (BSM) contributions could arise. One can obtain sensitivity to BSM physics from precise measurement of the decay amplitudes, especially the angular distribu-

Notre Dame, IN 46556, ^vUniversidad de Oviedo, E-33007 Oviedo, Spain, ^wTexas Tech University, Lubbock, TX 79609, ^xIFIC(CSIC-Universitat de Valencia), 56071 Valencia, Spain, ^yUniversidad Tecnica Federico Santa Maria, 110v Valparaiso, Chile, ^zUniversity of Virginia, Charlottesville, VA 22906, ^{aa}Yarmouk University, Irbid 211-63, Jordan, ⁱⁱOn leave from J. Stefan Institute, Ljubljana, Slovenia,

tions of the decay products.

The full differential decay distribution for the decay $B \rightarrow K^*(892)\mu^+\mu^- \rightarrow K\pi\mu^+\mu^-$ is described by four independent kinematic variables: the dimuon invariant mass squared $q^2 \equiv M_{\mu\mu}^2 c^2 (\text{GeV}^2/c^2)$, the angle θ_μ between the μ^+ (μ^-) direction and the direction opposite to the B (\bar{B}) meson in the dimuon rest frame, the angle θ_K between the kaon direction and the direction opposite to the B meson in the K^* rest frame, and the angle ϕ between the two planes formed by the dimuon and the K - π systems. The angle ϕ is zero if the two planes are parallel. The distributions of θ_μ , θ_K , and ϕ are projected from the full differential decay distribution and can be parametrized with four angular observables, A_{FB} , F_L , $A_T^{(2)}$, and A_{im} [1–5]:

$$\begin{aligned} \frac{1}{\Gamma} \frac{d\Gamma}{d \cos \theta_K} &= \frac{3}{2} F_L \cos^2 \theta_K + \frac{3}{4} (1 - F_L) (1 - \cos^2 \theta_K), \\ \frac{1}{\Gamma} \frac{d\Gamma}{d \cos \theta_\mu} &= \frac{3}{4} F_L (1 - \cos^2 \theta_\mu) + \frac{3}{8} (1 - F_L) (1 + \cos^2 \theta_\mu) \\ &\quad + A_{FB} \cos \theta_\mu, \\ \frac{1}{\Gamma} \frac{d\Gamma}{d\phi} &= \frac{1}{2\pi} \left[1 + \frac{1}{2} (1 - F_L) A_T^{(2)} \cos 2\phi + A_{im} \sin 2\phi \right], \end{aligned} \quad (1)$$

where $\Gamma \equiv \Gamma(B \rightarrow K^*\mu^+\mu^-)$, A_{FB} is the muon forward-backward asymmetry, F_L is the K^* longitudinal polarization fraction, $A_T^{(2)}$ is the transverse polarization asymmetry [1], and A_{im} is the time-reversal-odd charge-and-parity asymmetry (T -odd CP asymmetry) [2, 6]. In the case of \bar{B} decay, $\sin \phi$ has opposite sign to that of the B decay due to the flipped dimuon plane. Since A_{im} is a coefficient of the $\sin 2\phi$ term in Eq. (1), A_{im} is a measure of the CP asymmetry. Experimental access to these angular observables extends the sensitivity to a large class of BSM physics models

The differential decay distribution is calculated in an operator product expansion [7]. In the SM, the nonzero terms are parametrized by the short-distance Wilson coefficients $C_{7,9,10}^{\text{eff}}$. Since various BSM models predict couplings to the K^{*0} helicity states that are different from the SM ones, the measurement of F_L could constrain BSM parameters [1]. The SM prediction in the range $1 < q^2 < 6 \text{ GeV}^2/c^2$ is $F_L^{\text{SM}} = 0.73_{-0.03}^{+0.02}$ [3]. The quantity A_{FB} is expected to be small at low q^2 and to have a large positive value at high q^2 in the SM. In the range $1 < q^2 < 6 \text{ GeV}^2/c^2$, the SM predicts $A_{FB}^{\text{SM}} = 0.022 \pm 0.028$ [3]. The BSM contributions can change the magnitude and the sign of A_{FB} . For example, some BSM models such as supergravity models with large $\tan \beta$ [8] allow an opposite sign of C_7^{eff} compared to the SM, resulting in the opposite sign of A_{FB} at low q^2 . In the SM $A_T^{(2)}$ is expected to be approximately zero at low q^2 and negative at high q^2 [9]. Some BSM models like R -parity conserving minimal supersymmetry [10] predict the existence of right-handed currents. In such a case, $A_T^{(2)}$ could be enhanced up to ± 1 [1, 3, 11]. The SM

predicts the quantity A_{im} to be very close to zero for all accessible q^2 , and this quantity is particularly sensitive to the existence of CP violation in right-handed currents in BSM physics [5, 6].

BABAR [12], Belle [13], and CDF [14] have reported measurements of A_{FB} and F_L in the $B \rightarrow K^*\ell\ell$ decay modes. All experiments find A_{FB} to be larger than the SM expectation, but so far none has sufficient sensitivity to be conclusive. In this Letter, we report measurements of the angular distributions in the decay $B \rightarrow K^{(*)}\mu^+\mu^-$ using a data sample, corresponding to an integrated 6.8 fb^{-1} , of $p\bar{p}$ collisions at a center-of-mass energy of $\sqrt{s} = 1.96 \text{ TeV}$, collected with the CDF II detector between March 2002 and June 2010. The measurement updates and supersedes an earlier analysis on 4.4 fb^{-1} [14]. Besides the 54% increase in luminosity, we have added new decays channels $B^+ \rightarrow K^{*+}\mu^+\mu^-$ and improved the selection achieving a 9% increase in $B^0 \rightarrow K^{*0}\mu^+\mu^-$ signal efficiency with almost the same background rejection. The resulting factor of 82% increase in signal statistics allows us to access for the first time the angular observables $A_T^{(2)}$ and A_{im} in the decays $B \rightarrow K^*\mu^+\mu^-$. The measurements of the total and differential branching ratios of the $B \rightarrow K^{(*)}\mu^+\mu^-$ decays are reported in another letter [15].

The reconstruction of the $B \rightarrow K^{(*)}\mu^+\mu^-$ decays starts with a dimuon sample selected by the online trigger system [16] of the CDF II detector [17]. The trigger system uses information from muon detectors and the central drift tracking chamber. The central drift tracking chamber [18] provides 96 measurements per track between radii of 40 and 137 cm, allowing an accurate determination of the charged-particle momentum. The CMU and CMX muon drift chambers [19] cover the pseudorapidity regions $|\eta| < 0.6$ and $0.6 < |\eta| < 1.0$, respectively [20]. The CMP muon system is located radially behind the CMU and an additional steel absorber, and covers $|\eta| < 0.6$. The dimuon trigger requires a pair of oppositely charged tracks with momenta transverse to the beamline $p_T \geq 1.5 \text{ GeV}/c$, that are also identified in the CMU or CMX chambers. At least one of the muon tracks in the pair is required to be a CMU muon. The trigger also requires that either the dimuon pair satisfies $L_{xy} > 100 \mu\text{m}$, where the transverse decay length L_{xy} is the flight distance between the dimuon vertex and the event primary vertex and projected on the dimuon momentum vector, or that one of the muon candidates has $p_T > 3.0 \text{ GeV}/c$ and is identified by both CMU and CMP chambers. The other detector subsystems relevant for this analysis are discussed in Ref. [21]. Each offline track is required to satisfy the standard quality requirements (e.g. hits in the silicon detector) to ensure well measured momenta and decay vertices [14]. The decay length and invariant mass of each dimuon pair are calculated after a vertex fit using the muon tracks. Dimuons are required to have q^2 val-

ues outside the ranges of $8.68 < q^2 < 10.09 \text{ GeV}^2/c^2$ and $12.86 < q^2 < 14.18 \text{ GeV}^2/c^2$ [14], to be inconsistent with decays of either J/ψ or $\psi(2S)$ mesons, which are typically reconstructed with $14 \text{ MeV}/c^2$ mass resolution. The dimuon pair is then combined with charged tracks forming a $K^{*0} \rightarrow K^+\pi^-$ candidate to form a $B^0 \rightarrow K^{*0}\mu^+\mu^-$ candidate, or a $K^{*+} \rightarrow K_S^0(\rightarrow \pi^+\pi^-)\pi^+$ candidate to form a $B^+ \rightarrow K^{*+}\mu^+\mu^-$ candidate. Charge-conjugate modes are implied throughout this Letter. The K_S^0 , K^{*0} , and K^{*+} candidates are required to have reconstructed invariant masses consistent with the world average values [22], and to have $p_T > 1 \text{ GeV}/c$. The K_S^0 is also required to have its decay vertex displaced from the dimuon vertex. The ambiguity in the mass assignment of the decay products in the $K^{*0} \rightarrow K^+\pi^-$ decay is handled by choosing the combination whose $K^+\pi^-$ mass is closest to the world average K^{*0} mass, which is correct in approximately 92% of cases. The reconstructed B candidates are required to have $p_T > 4 \text{ GeV}/c$. To further optimize the event selection, an artificial neural network (NN) classifier is trained for each channel using simulated signal events and background events taken from mass sidebands in data. Simulated signal distributions are corrected using scale factors extracted by comparing simulation to data in the control samples $B \rightarrow J/\psi(\rightarrow \mu^+\mu^-)K^{(*)}$. The optimized NN threshold is determined to minimize the statistical uncertainty of the angular observables, using many kinematic observables including p_T , invariant mass, vertex fit parameters, and muon identification quality [14].

The signal yield is obtained by an unbinned maximum likelihood fit to the invariant mass distribution with a probability density function (PDF) consisting of Gaussian distributions for the signal and a linear background. We find a total of 234 ± 19 $B^+ \rightarrow K^+\mu^+\mu^-$, 164 ± 15 $B^0 \rightarrow K^{*0}\mu^+\mu^-$, and 20 ± 6 $B^+ \rightarrow K^{*+}\mu^+\mu^-$ events. We divide the signal region into six bins in q^2 . Two semi-inclusive bins are included with ranges covering theoretically well-controlled regions. We obtain the signal yields in the individual q^2 ranges by fitting the invariant mass in a similar way. The resulting yields are listed in Tables I, II, and III. The invariant mass distributions are shown in Fig. 1.

To extract the quantities F_L , A_{FB} , $A_T^{(2)}$, and A_{im} , we perform likelihood fits to distributions of $\cos\theta_K$, $\cos\theta_\mu$, and ϕ for events in each q^2 range. The signal fractions are fixed to the values obtained from the invariant mass fits. Signal PDFs for angular distributions are formed from Eq. (1), taking into account the estimation of the detector acceptance of the decay angles and the K - π interchange using Monte Carlo simulations. The incorrect K - π assignment in the $K^{*0} \rightarrow K^+\pi^-$ decay distorts the signal mass distribution and swaps the sign of $\cos\theta_\mu$. This effect is taken into account by introducing an additional signal-like term into the likelihood function. The contribution from decays with non-resonant K - π pairs is

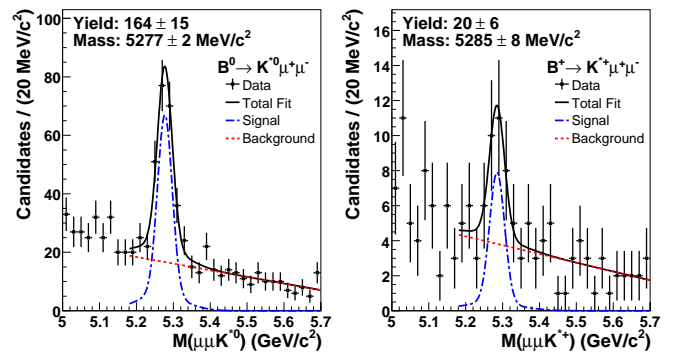


FIG. 1: Invariant mass of $B^0 \rightarrow K^{*0}\mu^+\mu^-$ (left) and $B^+ \rightarrow K^{*+}\mu^+\mu^-$ (right), with fit results overlaid.

estimated to be small [1] and neglected in the fit. The background PDF shapes for the angular distributions are modeled from events in the B mass sidebands. The values of F_L in individual q^2 ranges are extracted from fits to the $\cos\theta_K$ distributions and then used as inputs in the determinations of the other three observables. The asymmetry A_{FB} is obtained from fits to the $\cos\theta_\mu$ distributions, and $A_T^{(2)}$ and A_{im} are from fits to the ϕ distributions.

The extracted observables in the decay mode $B^0 \rightarrow K^{*0}\mu^+\mu^-$ are listed in Table I, and the forward-backward asymmetry A_{FB} is illustrated in Fig. 2(a) as a function of q^2 . To increase sensitivity, we also perform a fit to the combined $B^0 \rightarrow K^{*0}\mu^+\mu^-$ and $B^+ \rightarrow K^{*+}\mu^+\mu^-$ modes, assuming they have the same decay dynamics. The combined fit results are listed in Table II and shown in Fig. 3. On average A_{FB} resolutions are improved by factors of 1.5 (1.8) times from previous CDF measurement [14] for $B^0 \rightarrow K^{*0}\mu^+\mu^-$ ($B \rightarrow K^*\mu^+\mu^-$). The current data are consistent with the SM and with the inverted C_7 scenario. In addition, a new measurement of A_{FB} in the decay $B^+ \rightarrow K^+\mu^+\mu^-$ is obtained. In the SM, the expected value of A_{FB} for this mode is quite small over the entire range of q^2 [23], whereas some BSM models predict enhanced values of A_{FB} [11]. In the A_{FB} fit, we assume no scalar term [23] and set $F_L = 1$. The result is shown in Fig. 2(b) and listed in Table III. The current data is consistent with the SM.

The sources of systematic uncertainty in the angular observables include the estimation of detector acceptance of the decay angles, signal fraction estimation and shape modeling of events in the signal window, feed-down background from other B decays, trigger efficiency and bias modeling, incorrect K - π assignment in the $K^{*0} \rightarrow K^+\pi^-$ decay, and fitting bias. The largest contribution is that from uncertainties on the signal fraction in the signal window. The total systematic uncertainties on the asymmetry observables for various q^2 values are in the ranges $0.02 - 0.09$ for F_L , $0.05 - 0.17$ for A_{FB} , $0.07 - 2.21$ for $A_T^{(2)}$,

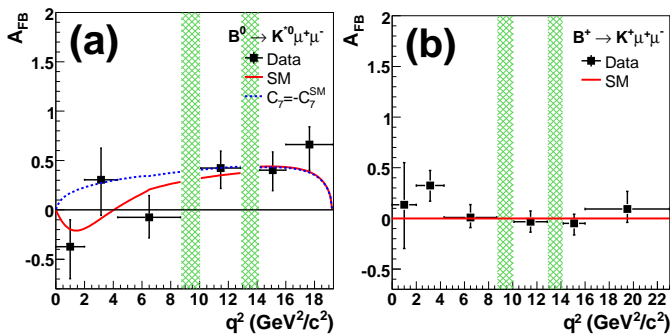


FIG. 2: Measurements of forward-backward asymmetry A_{FB} in the decay (a) $B^0 \rightarrow K^{*0} \mu^+ \mu^-$ and (b) $B^+ \rightarrow K^+ \mu^+ \mu^-$ as a function of dimuon mass squared q^2 . Points are the fit results from data. The solid curves are the SM expectation [24]. The dotted curve is the $C_7 = -C_7^{\text{SM}}$ expectation suggested by some BSM models. Hatched regions are excluded resonant (charmonium) decay regions.

and $0.01 - 0.14$ for A_{im} in the mode $B^0 \rightarrow K^{*0} \mu^+ \mu^-$. Similar sizes of systematic uncertainties are found in the combined fit results.

In summary, we have reconstructed the decays $B^0 \rightarrow K^{*0} \mu^+ \mu^-$ and $B^+ \rightarrow K^+ \mu^+ \mu^-$ and measured their angular distributions. We have measured the muon forward-backward asymmetry A_{FB} , the K^* longitudinal polarization fraction F_L , the transverse polarization asymmetry $A_T^{(2)}$, and the T -odd CP asymmetry A_{im} as a function of the dimuon mass squared q^2 . Measurements of $A_T^{(2)}$ and A_{im} are reported for the first time. The muon forward-backward asymmetry A_{FB} is also measured in the decay mode $B^+ \rightarrow K^+ \mu^+ \mu^-$ and represents an update with higher precision. All of the new reported results presented in this Letter are among the most accurate to date and consistent with the SM predictions, but still statistically limited in providing stringent tests on various models. The results are also consistent with recent measurements from B -factory experiments [12, 13].

We wish to tender our cordial thanks to Christoph Bobeth, Joaquim Matias, and Wolfgang Altmannshofer, for close communication and valuable suggestions about the angular observables. We express our special gratitude to Danny van Dyk, who provided the tool to obtain the theoretical predictions for the angular observables.

We thank the Fermilab staff and the technical staffs of the participating institutions for their vital contributions. This work was supported by the U.S. Department of Energy and National Science Foundation; the Italian Istituto Nazionale di Fisica Nucleare; the Ministry of Education, Culture, Sports, Science and Technology of Japan; the Natural Sciences and Engineering Research Council of Canada; the National Science Council of the Republic of China; the Swiss National Science Foundation; the A.P. Sloan Foundation; the Bundesministerium

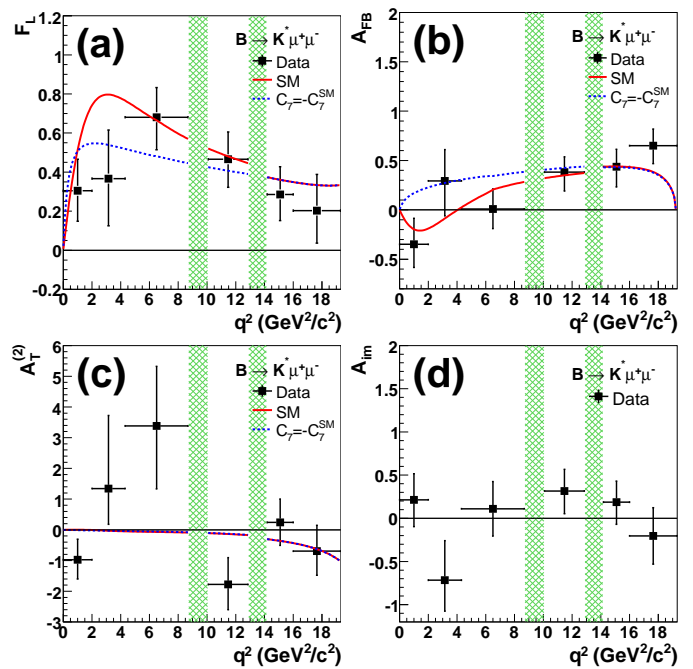


FIG. 3: Measurements of (a) longitudinal K^* polarization fraction F_L , (b) forward-backward asymmetry A_{FB} , (c) transverse polarization asymmetry $A_T^{(2)}$, and (d) T -odd CP asymmetry A_{im} in the combined decay mode $B \rightarrow K^* \mu^+ \mu^-$, all presented as a function of dimuon mass squared q^2 . The points are the fit results from data. The solid curves are the SM expectation [24]. The dotted curves are the $C_7 = -C_7^{\text{SM}}$ expectation. Hatched regions are resonant (charmonium) decay regions.

für Bildung und Forschung, Germany; the Korean World Class University Program, the National Research Foundation of Korea; the Science and Technology Facilities Council and the Royal Society, UK; the Institut National de Physique Nucleaire et Physique des Particules/CNRS; the Russian Foundation for Basic Research; the Ministerio de Ciencia e Innovación, and Programa Consolider-Ingenio 2010, Spain; the Slovak R&D Agency; and the Academy of Finland.

-
- [1] F. Kruger and J. Matias, Phys. Rev. D **71**, 094009 (2005).
 - [2] U. Egede *et al.*, J. High Energy Phys. 11 (2008) 032.
 - [3] S. Descotes-Genon *et al.*, J. High Energy Phys. 06 (2011) 099.
 - [4] F. Kruger *et al.*, Phys. Rev. D **61**, 114028 (2000).
 - [5] W. Altmannshofer *et al.*, J. High Energy Phys. 01 (2009) 019.
 - [6] C. Bobeth, G. Hiller, and G. Piranishvili, J. High Energy Phys. 07 (2008) 106.
 - [7] K. G. Wilson, Phys. Rev. **179**, 1499 (1969).
 - [8] A. Ali *et al.*, Phys. Rev. D **61**, 074024 (2000).
 - [9] C. Bobeth, G. Hiller, and D. van Dyk, J. High Energy

TABLE I: Summary of $B^0 \rightarrow K^{*0} \mu^+ \mu^-$ fit results. First (second) uncertainty is statistical (systematic).

q^2 (GeV ² /c ²)	$N(K^{*0} \mu^+ \mu^-)$	F_L	A_{FB}	$A_T^{(2)}$	A_{im}
[0.00, 2.00)	30.7 ± 4.7	$0.31^{+0.17}_{-0.16} \pm 0.02$	$-0.37^{+0.27}_{-0.32} \pm 0.11$	$-0.8 \pm 0.7 \pm 0.3$	$0.37^{+0.31}_{-0.33} \pm 0.08$
[2.00, 4.30)	14.2 ± 4.2	$0.35^{+0.26}_{-0.24} \pm 0.03$	$0.30^{+0.32}_{-0.36} \pm 0.17$	$1.4^{+2.0}_{-1.1} \pm 1.2$	$-0.80^{+0.48}_{-0.29} \pm 0.13$
[4.30, 8.68)	31.3 ± 7.4	$0.60^{+0.17}_{-0.18} \pm 0.05$	$-0.08^{+0.22}_{-0.21} \pm 0.03$	$1.8^{+1.6}_{-1.7} \pm 1.5$	$0.03^{+0.34}_{-0.34} \pm 0.06$
[10.09, 12.86)	38.4 ± 7.6	$0.40^{+0.16}_{-0.16} \pm 0.02$	$0.42^{+0.17}_{-0.21} \pm 0.10$	$-1.0^{+0.9}_{-0.8} \pm 0.5$	$0.47^{+0.26}_{-0.28} \pm 0.09$
[14.18, 16.00)	31.6 ± 4.7	$0.32^{+0.14}_{-0.14} \pm 0.03$	$0.40^{+0.18}_{-0.21} \pm 0.07$	$0.4 \pm 0.8 \pm 0.2$	$0.15^{+0.25}_{-0.26} \pm 0.01$
[16.00, 19.30)	20.7 ± 4.8	$0.16^{+0.22}_{-0.18} \pm 0.06$	$0.66^{+0.18}_{-0.26} \pm 0.19$	$-0.9 \pm 0.8 \pm 0.4$	$-0.30^{+0.36}_{-0.35} \pm 0.14$
[0.00, 4.30)	44.2 ± 6.5	$0.33^{+0.14}_{-0.14} \pm 0.02$	$-0.08^{+0.21}_{-0.20} \pm 0.05$	$-0.2 \pm 0.6 \pm 0.1$	$-0.02^{+0.28}_{-0.28} \pm 0.01$
[1.00, 6.00)	23.8 ± 6.5	$0.60^{+0.21}_{-0.23} \pm 0.09$	$0.36^{+0.46}_{-0.28} \pm 0.11$	$1.6^{+1.8}_{-1.9} \pm 2.2$	$-0.02^{+0.40}_{-0.40} \pm 0.03$

TABLE II: Summary of combined $B \rightarrow K^* \mu^+ \mu^-$ fit results. First (second) uncertainty is statistical (systematic). $N(K^{*0} \mu^+ \mu^-)$ is taken from Table I.

q^2 (GeV ² /c ²)	$N(K^{*+} \mu^+ \mu^-)$	F_L	A_{FB}	$A_T^{(2)}$	A_{im}
[0.00, 2.00)	2.5 ± 1.6	$0.30^{+0.16}_{-0.16} \pm 0.02$	$-0.35^{+0.26}_{-0.23} \pm 0.10$	$-1.0^{+0.7}_{-0.6} \pm 0.4$	$0.21^{+0.30}_{-0.31} \pm 0.10$
[2.00, 4.30)	1.3 ± 1.8	$0.37^{+0.25}_{-0.24} \pm 0.10$	$0.29^{+0.32}_{-0.35} \pm 0.15$	$1.3^{+2.4}_{-1.2} \pm 0.9$	$-0.72^{+0.46}_{-0.36} \pm 0.21$
[4.30, 8.68)	3.9 ± 3.5	$0.68^{+0.15}_{-0.17} \pm 0.09$	$0.01^{+0.20}_{-0.20} \pm 0.09$	$3.4^{+1.9}_{-2.1} \pm 3.6$	$0.11^{+0.31}_{-0.32} \pm 0.09$
[10.09, 12.86)	6.0 ± 2.8	$0.47^{+0.14}_{-0.14} \pm 0.03$	$0.38^{+0.16}_{-0.19} \pm 0.09$	$-1.8^{+0.9}_{-0.8} \pm 0.8$	$0.32^{+0.25}_{-0.26} \pm 0.06$
[14.18, 16.00)	1.6 ± 1.8	$0.29^{+0.14}_{-0.13} \pm 0.05$	$0.44^{+0.18}_{-0.21} \pm 0.10$	$0.2 \pm 0.8 \pm 0.2$	$0.19^{+0.24}_{-0.26} \pm 0.04$
[16.00, 19.30)	4.1 ± 2.3	$0.20^{+0.19}_{-0.17} \pm 0.05$	$0.65^{+0.17}_{-0.18} \pm 0.16$	$-0.7 \pm 0.8 \pm 0.3$	$-0.20^{+0.33}_{-0.33} \pm 0.09$
[0.00, 4.30)	3.8 ± 2.4	$0.33^{+0.14}_{-0.13} \pm 0.03$	$-0.08^{+0.21}_{-0.20} \pm 0.05$	$-0.3 \pm 0.6 \pm 0.1$	$-0.10^{+0.27}_{-0.26} \pm 0.10$
[1.00, 6.00)	5.0 ± 3.0	$0.69^{+0.19}_{-0.21} \pm 0.08$	$0.29^{+0.20}_{-0.23} \pm 0.07$	$1.7 \pm 2.2 \pm 2.5$	$0.09^{+0.34}_{-0.35} \pm 0.18$

TABLE III: Summary of $B^+ \rightarrow K^+ \mu^+ \mu^-$ fit results.

q^2 (GeV ² /c ²)	$N(K^+ \mu^+ \mu^-)$	A_{FB}
[0.00, 2.00)	18.6 ± 5.6	$0.13^{+0.42}_{-0.43} \pm 0.07$
[2.00, 4.30)	40.3 ± 6.7	$0.32^{+0.15}_{-0.16} \pm 0.05$
[4.30, 8.68)	68.5 ± 10.5	$0.01^{+0.13}_{-0.10} \pm 0.01$
[10.09, 12.86)	43.5 ± 7.1	$-0.03^{+0.11}_{-0.10} \pm 0.04$
[14.18, 16.00)	35.9 ± 5.7	$-0.05^{+0.09}_{-0.11} \pm 0.03$
[16.00, 23.00)	28.9 ± 6.3	$0.09^{+0.17}_{-0.13} \pm 0.03$
[0.00, 4.30)	57.8 ± 8.8	$0.31^{+0.16}_{-0.16} \pm 0.04$
[1.00, 6.00)	74.5 ± 9.6	$0.13^{+0.09}_{-0.09} \pm 0.02$

Phys. 07 (2010) 098.

- [10] E. Lunghi and J. Matias, J. High Energy Phys. 04 (2007) 058.
- [11] A. K. Alok *et al.*, arXiv:1008.2367 (2010).
- [12] B. Aubert *et al.* (BaBar Collaboration), Phys. Rev. D **79**, 031102 (2009).
- [13] J. T. Wei *et al.* (Belle Collaboration), Phys. Rev. Lett. **103**, 171801 (2009).
- [14] T. Aaltonen *et al.* (CDF Collaboration), Phys. Rev. Lett. **106**, 161801 (2011).
- [15] T. Aaltonen *et al.* (CDF Collaboration), arXiv:1107.3753 (2011).
- [16] E. J. Thomson *et al.*, IEEE Trans. Nucl. Sci. **49**, 1063 (2002).
- [17] D. Acosta *et al.* (CDF Collaboration), Phys. Rev. D **71**, 032001 (2005).
- [18] A. A. Affolder *et al.* (CDF Collaboration), Nucl. Instrum. Methods A **526**, 249 (2004).
- [19] G. Ascoli *et al.*, Nucl. Instrum. Methods A **268**, 33 (1988); T. Dorigo (CDF Collaboration), Nucl. Instrum. Methods A **461**, 560 (2001).
- [20] We use a cylindrical coordinate system in which θ is the polar angle with respect to the proton beamline and pseudorapidity $\eta \equiv -\ln(\tan \theta/2)$.
- [21] T. Aaltonen *et al.* (CDF Collaboration), Phys. Rev. Lett. **102**, 242002 (2009), and references therein.
- [22] K. Nakamura *et al.* (Particle Data Group), J. Phys. G **37**, 075021 (2010).
- [23] C. Bobeth, G. Hiller, and G. Piranishvili, J. High Energy Phys. 12 (2007) 040.
- [24] We draw theory curves using the EOS code by D. van Dyk *et al.* (<http://project.het.physik.tu-dortmund.de/eos/>). However, for illustration purposes, we extend these curves into kinematical regions ($q^2 < 1$, $7 < q^2 < 8.68$, $10.09 < q^2 < 12.86$) where their reliability is known to be approximate.